PERGAMON

European Journal of Cancer 37 (2001) 131–139

European Journal of Cancer

www.ejconline.com

Biodistribution and antitumour efficacy of long-circulating N-(2-hydroxypropyl)methacrylamide copolymer–doxorubicin conjugates in nude mice

J.-G. Shiah [a], M. Dvořák, P. Kopečková [a], Y. Sun [c], C.M. Peterson [b], J. Kopeček [a,*]

[a] *Department of Pharmaceutics and Pharmaceutical Chemistry/CCCD, University of Utah, Salt Lake City, UT 84112, USA*
[b] *Department of Obstetrics and Gynecology, University of Utah, Salt Lake City, UT 84112, USA*
[c] *Utah Center for Photomedicine, VA Medical Center, Salt Lake City, UT 84112, USA*

Received 10 July 2000; received in revised form 8 August 2000; accepted 16 August 2000

Abstract

The aim of this study was to evaluate the influence of the molecular weight (mol. wt) of N-(2-hydroxypropyl)methacrylamide (HPMA) copolymer–doxorubicin (DOX) conjugates (P-DOX) on biodistribution and therapeutic efficacy in nu/nu mice bearing human ovarian carcinoma OVCAR-3 xenografts. Copolymerisation of HPMA, a polymerisable derivative of DOX (N-methacryloylglycylphenylalanylleucylglycyl doxorubicin) and a newly designed crosslinking agent, N^2,N^5-bis(N-methacryloylglycylphenylalanyl-leucylglycyl)ornithine methyl ester monomers resulted in novel, high mol. wt, branched, water-soluble P-DOX containing lysosomally degradable oligopeptide sequences as crosslinks and side-chains terminated in DOX. Four conjugates with mol. wt of 22, 160, 895 and 1230 kDa were prepared. The results indicated that the half-life in blood and the elimination rate from the tumour were up to 28 times longer and 25 times slower, respectively, for P-DOX (mol. wt = 1230 kDa) than for free DOX. Treatment with P-DOX (mol. wt $\geqslant$ 160 kDa) inhibited tumour growth more efficiently than that of 22 kDa P-DOX or free DOX ($P < 0.02$) at a 2.2 mg/kg DOX equivalent dose. In conclusion, the administration of long circulating P-DOX resulted in enhanced tumour accumulation with a concomitant increase in therapeutic efficacy.

Keywords: Doxorubicin; EPR effect; Long-circulating conjugate; N-(2-hydroxypropyl)methacrylamide copolymer; Ovarian carcinoma

1. Introduction

Macromolecular therapeutics possess features distinctive from low-molecular weight drugs [1]. The main factor responsible is the change of the mechanism of cell entry. Whereas low-molecular weight drugs enter cells by diffusion, macromolecular therapeutics are internalised by endocytosis and ultimately localised in the lysosomal compartment of the cell [2]. N-(2-Hydroxypropyl)methacrylamide (HPMA) copolymers containing oligopeptide side-chains as drug attachment/release points have been proposed as macromolecular therapeutics [3]. In fact, the HPMA copolymer–doxorubicin (DOX) conjugate has shown remarkable results in phase I clinical trials [4].

Molecular weight (mol. wt) and molecular weight distribution of drug carriers have an impact on their efficacy in the treatment of solid tumours. High-molecular weight (long-circulating) polymeric carriers accumulate efficiently in tumour tissue [5–7] due to the enhanced permeability and retention (EPR) effect [8]. However, if they possess a non-degradable backbone, they may deposit and accumulate in various organs [9]. We have recently designed a reproducible synthetic pathway for high-molecular weight (branched) water-soluble HPMA copolymer–DOX conjugates (P-DOX) containing lysosomally degradable oligopeptide crosslinks, as well as side-chains terminating in DOX [10]. Such conjugates would release DOX in the lysosomal compartment and, in addition, be degraded there to primary chains that can be eliminated from the organism after tumour cell death, if their size is below the renal threshold.

We hypothesise that high-mol. wt P-DOX conjugates will be preferentially accumulated in solid tumours and

* Corresponding author. Tel.: +1-801-581-4532; fax: +1-801-581-3674.
E-mail address: jindrich.kopecek@m.cc.utah.edu (J. Kopeček).

0959-8049/01/$ - see front matter
PII: S0959-8049(00)00374-9

their antitumour efficacy will be mol. wt-dependent. To verify the hypothesis, four long-circulating P-DOX conjugates of different mol. wt (range: 22–1230 kDa) were administered intravenously (i.v.) to nu/nu mice bearing OVCAR-3 human ovarian carcinoma xenografts. Their biodistribution and efficacy in the tumour treatment of the conjugates were studied.

2. Materials and methods

2.1. Materials

Daunorubicin was from the Sigma Chemical Co., St Louis, MO, USA. Doxorubicin was a generous gift from A. Suarato, Pharmacia-Upjohn, Milano, Italy. They were used as received without further purification. All the organic solvents used for the assay were high performance liquid chromatography (HPLC) grade.

Sorensen's glycine buffer of pH 2.6 was prepared by mixing 0.1 M glycine/NaCl and 0.1 M HCl in double distilled water to make a 10 mM buffer. The pH was monitored by a Corning pH meter model 340, calibrated with Corning standard buffers.

2.2. Syntheses of HPMA Copolymer–DOX conjugates

The HPMA copolymer–DOX conjugates (P-DOX) with different mol. wt were prepared by copolymerising HPMA, polymerisable N-methacryloylglycylphenylalanylleucylglycyl doxorubicin, and crosslinking agent N^2,N^5 - bis(N - methacryloylglycylphenylalanylleucylglycyl)ornithine methyl ester monomers in a methanol/dimethyl sulphoxide (DMSO) solution using 2,2′-azobisisobutyronitrile as the initiator, as previously described [10]. The polymerisation mixture was purged with nitrogen and sealed in an ampoule. The polymerisation proceeded for 24 h at 50°C, the polymer was isolated by precipitation into acetone/ether, filtered off, and dried under vacuum. The DOX content in the conjugates was determined by ultraviolet (UV) spectroscopy. The mol. wt was determined by size exclusion chromatography using a fast performance liquid chromatography (FPLC) system (Pharmacia) equipped with a Sephacryl S-500 HR or Superose 6 column and a light scattering detector (MiniDawn®), Wyatt Technology Corporation, Santa Barbara, CA, USA calibrated with poly(HPMA) fractions in phosphate-buffered solution (PBS) buffer (pH 7.3).

2.3. Animal model

Female nu/nu athymic mice (5–6 weeks; 15–17 g; Simonsen Laboratories, Inc., Gilroy, CA, USA) were cared for under the guidelines of an approved protocol from the University of Utah Institutional Animal Care and Use Committee. They were accommodated in a pathogen-free laboratory environment for 2 weeks before the initiation of any treatment. The OVCAR-3 carcinoma was maintained subcutaneously (s.c.) in nu/nu mice, and tumours were s.c. implanted into mice, as previously described [11]. Experiments were initiated when a consistent growth rate and a tumour volume of $\geqslant 20$ mm^3 were achieved [11,12].

2.4. Biodistribution study

Animals received a single i.v. injection of free DOX or P-DOX solution at a DOX equivalent dose of 1 mg/kg in bacteriostatic 0.9% NaCl solution. The mice (three per group) were killed at 2, 6, 12, 18 and 24 h (for free DOX) and at 12, 24, 36, 48, and 168 h (for P-DOX) after administration of the drug solution. The tissues, including heart, lung, liver, spleen, kidney and tumour, were harvested without perfusion, lyophilised and weighed. Blood was also collected for evaluation.

2.5. Determination of DOX level in tissues

The DOX concentration in blood and tissues was determined by an HPLC-fluorescence assay [6]. In brief, lyophilised tissues were homogenised into 15 mg/ml solutions in a 0.2 M sodium phosphate buffer at pH 7.4 for 18 h in an incubator. An appropriate amount of daunorubicin as the internal standard was added to each sample (0.7 ml) followed by the addition of silver nitrate (100 μl, 0.1 M). Triple extraction was performed after adding chloroform:isopropanol (3:1; v:v; total 0.9 ml) and vigorous vortex-mixing. The organic layers were collected after centrifugation at 16 000*g* for 15 min at room temperature, combined, and filtered to remove all particulate materials. The solutions were evaporated to dryness, and redissolved in a mobile phase solution (methanol: isopropanol: Sorensen's buffer; 10:20:70; v:v:v). The sample solution was then applied to a Dionex HPLC system (Dionex Corp., Sunnyvale, CA, USA) equipped with a Microsorb-MV C18 column (Varian Chromatography Systems, Walnut Creek, CA, USA) and a Waters™ 474 scanning fluorescence detector (Waters, Milford, MA, USA) under isocratic conditions. The fluorescence intensity was recorded at an excitation wavelength ($\lambda_{exc.}$) = 480 nm and an emission wavelength (λ_{emi}) = 560 nm. A similar assay (as used for free DOX) was used for the quantitative analysis of P-DOX concentrations in tissues, except that the samples of P-DOX were subjected to an optimised acid hydrolysis (2 M HCl at 85°C for 10 min) before extraction [6]. The DOX concentrations in blood or tissue samples were determined using calibration curves established by adding free DOX or P-DOX solution of known concentrations to the blood or respective tissues harvested from control mice receiving bacteriostatic 0.9% NaCl solution.

Table 1
Characteristics of P-DOX conjugates

Conjugate mol. wt (kDa)	Polydispersity	DOX content (mole %)	DOX content (weight %)
22	1.3	1.38	5.25
160	3.6	1.34	5.1
895	3.3	1.14	4.34
1230	5.2	1.01	3.84

Polydispersity = weight-averaged molecular weight/number-averaged molecular weight. DOX, doxorubicin.

2.6. Bioactivity evaluation

The bioactivity of P-DOX was evaluated in nude mice bearing s.c. OVCAR-3 xenografts after a single i.v. administration of P-DOX solution at a DOX equivalent dose of 2.2 mg/kg. The control mice received saline buffer. Tumour size was monitored every 2–4 days for up to 34 days. The day that mice received drug solutions was set as day 0 and the tumour volume was normalised to 100%. All subsequent tumour volumes were then expressed as the percentage relative to those at day 0. Ellipsoidal tumour volumes were calculated using the formula: $(4/3)\pi a^2 b$, where a and b are the minimal and maximal radius of an ellipse, respectively [12]. A mean standard error was calculated for each experimental point. There were six mice in each group. The heartbeat was monitored by a *500* A Doppler (Multigon Industries, Inc., NJ, USA).

3. Results

3.1. Characteristics of HPMA copolymer–DOX conjugates

The N^2,N^5-bis(N-methacryloylglycylphenylalanylleucylglycyl)ornithine methyl ester crosslinking agent permits the synthesis of P-DOX conjugates with various mol. wts. The characteristics of the obtained conjugates, including the mol. wt, polydispersity, drug content in moles and weight per cent, are summarised in Table 1. The chemical structure of the conjugates is shown in Fig. 1.

3.2. Biodistribution

The HPLC chromatograms possessed distinct elution peaks, consistent with published reports [6], indicating that the protocol used to determine drug concentrations in extracts of blood or tissue samples was appropriate.

DOX levels in the blood after the mice received a single i.v. injection of free DOX or P-DOX solution are shown in Fig. 2. The levels of free DOX in the blood were 4.1 μg/g at 2 h, 0.3 μg/g at 12 h, and decreased to a barely detectable level at 24 h. In contrast, the concentration of P-DOX in the blood was much higher, and after 12 h following administration reached values of 2.3, 7.6, 13.2 and 24.7 μg/g for P-DOX of mol. wt 22, 160, 895 and 1230 kDa, respectively. Seven days (168 h) after administration, the concentration of P-DOX in the blood dropped to 1.2, 1.3 and 1.5 μg/g for conjugates with mol. wts of 160, 895 and 1230 kDa, respectively; only a background intensity was obtained for the P-DOX conjugate with a mol. wt of 22 kDa. As shown in Fig. 2, the calculated area under the curve (AUC) was 168 μg·h/g for free DOX, and 439 μg·h/g for P-DOX with a mol. wt of 22 kDa. A further increase of the mol. wt of P-DOX from 160 kDa to 1230 kDa resulted in an increase of the AUC in the blood from 803 μg×h/g to 1773 μg×h/g, respectively.

Assuming a first-order clearance model applied to the blood compartment following i.v. injection of free DOX or P-DOX into mice, the clearance rate constant Kc can be fitted; the results are shown in Fig. 3. The Kc of free DOX was obviously higher than that of P-DOX, and as the mol. wt of P-DOX increased, the Kc decreased, thus increasing the circulation half-life ($t_{1/2}$) in the blood. In this study, the $t_{1/2}$ of free DOX was approximately 30 min, while that of P-DOX with a mol. wt of 22 kDa was 2.6 h, consistent with our previous studies [6]. A further increase of the mol. wt of the conjugate from 160 to 1230 kDa extended the $t_{1/2}$ from 4.3 to 13.9 h.

The DOX level in the tumours after administration of free DOX or P-DOX is shown in Fig. 4. After i.v. administration of free DOX to the nude mice, the concentration of DOX in the tumours reached a peak level of 0.9 μg/g at 2 h, and it quickly dropped to 0.2 μg/g at 12 h and to an imperceptible concentration at 24 h. In contrast, the level of P-DOX in the tumours increased with time and mol. wt over the first 12 h after administration. The concentration reached levels of 0.5, 1.8, 2.8 and 2.8 μg/g at 24 h, and decreased at day 7 (168 h) to approximately 0, 0.7, 1.3 and 1.5 μg/g for P-DOX with a mol. wt of 22, 160, 895 and 1230 kDa, respectively. The peak level in the tumours shifted from 12 to 36 h as the mol. wt of P-DOX increased from 22 to 1230 kDa. The AUC of free DOX was calculated as 8.0 μg×h/g, and that for P-DOX at a mol. wt of 22, 160, 895 and 1230 kDa was 28.1, 189.2, 295 and 366 μg×h/g, respectively.

If a one-compartment model is suitable to describe the tumour accumulation of free DOX and P-DOX after i.v. injection into mice, then the first order accumulation rate constant K_a and elimination rate constant K_e can be determined [6]. The results are shown in Fig. 5. The K_a and K_e of free DOX are substantially larger than for P-DOX at a mol. wt greater than 22 kDa. However, as the mol. wt of P-DOX was equal to or greater than 160 kDa, the difference in K_a and K_e became minimal.

The levels of DOX in other tissues, including heart, kidney, liver, lung and spleen, after the administration

of free DOX or P-DOX to mice are summarised in Tables 2–6. The results for free DOX and P-DOX (mol. wt = 22 kDa) were in agreement with our previous study [6]. A significantly lower amount of P-DOX was found in the heart than free DOX, although the accumulation of P-DOX in the hearts increased as the mol. wt increased. The DOX concentration in the liver was 23.7 μg/g for P-DOX (mol. wt = 1230 kDa) 12 h after administration, and gradually decreased to approximately 9.6 μg/g at 48 h. After administration of free DOX, the concentration in the liver was lower than 5 μg/g at all time-points studied. The spleen accumulated DOX to a comparable level as the liver after administration of both, free DOX or P-DOX although the levels were generally slightly lower in the spleen following the administration of P-DOX. When compared with free DOX, the administration of P-DOX resulted in similar or slightly lower concentrations of DOX in the kidneys and lungs; the accumulation level increased with increasing mol. wt of P-DOX.

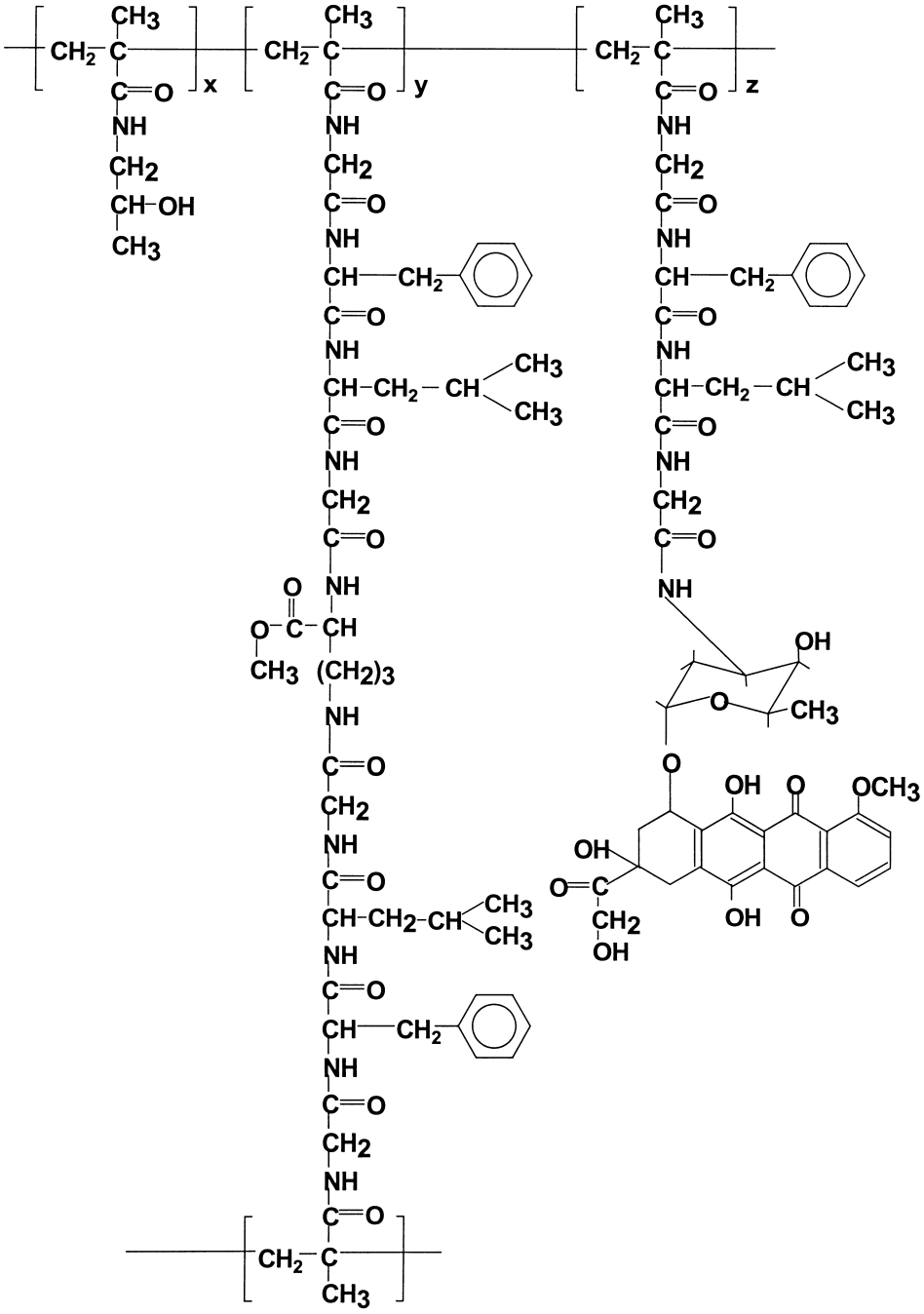

Fig. 1. Chemical structure of N-(2-hydroxypropyl)methacrylamide (HPMA) copolymer–doxorubicin conjugate containing glycylphenylalanylleucylglycine side-chains and the N^2,N^5-bis(N-methacryloylglycylphenylalanylleucylglycyl)ornithine crosslinker.

3.3. Therapeutic effect

The therapeutic efficacy of P-DOX toward OVCAR-3 human ovarian carcinoma xenografts in nude mice is shown in Fig. 6. A DOX equivalent dose of 2.2 mg/kg was used as in previous studies [11,12]. All tumours in the treatment groups exhibited more significant responses than those in the controls (all $P < 0.004$). The mice receiving P-DOX with a mol. wt equal to or higher than 160 kDa inhibited the tumour growth better than that of P-DOX with a mol. wt of 22 kDa (all $P < 0.02$). However, no statistical differences in tumour volumes

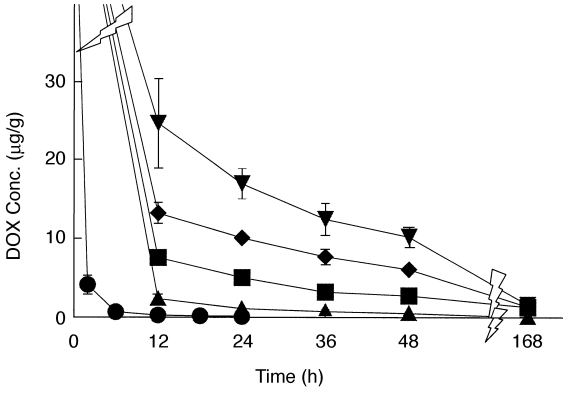

Fig. 2. Concentration of doxorubicin (DOX) in the blood of nu/nu mice after intravenous (i.v.) bolus injection of free DOX (●) or P-DOX of different mol. wts: 22 kDa (▲); 160 kDa (■); 895 kDa (◆); 1230 kDa (▼).

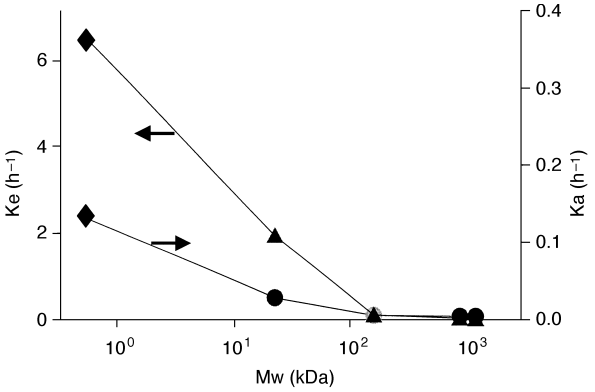

Fig. 5. Dependence of accumulation-elimination rate constants (K_a–K_e) on the mol. wt of P-DOX. K_a: (●); K_e: (▲). Free doxorubicin (DOX) (◆) is shown for comparison.

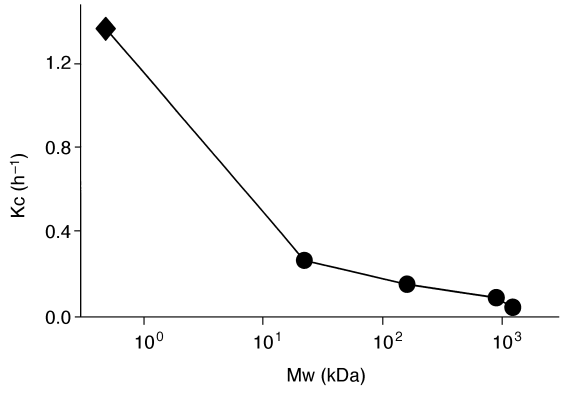

Fig. 3. Dependence of clearance rate constant K_c on the mol. wt of P-DOX (●). Free doxorubicin (DOX) (◆) was shown for comparison.

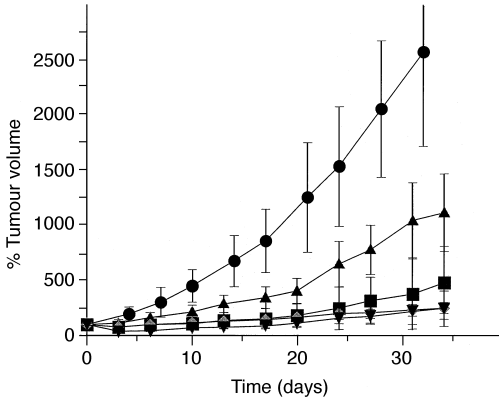

Fig. 6. Growth inhibition of subcutaneous (s.c.) human ovarian OVCAR-3 carcinoma xenografts in nu/nu mice by long-circulating P-DOX conjugates. The mice received intravenous (i.v.) injections of 2.2 mg/kg doxorubicin (DOX) equivalent dose: control (saline) (●); 22 kDa (▲); 160 kDa (■); 895 kDa (◆); and 1230 kDa (▲). $n = 6$ in each group. Values are the means ± the standard deviations (S.D.).

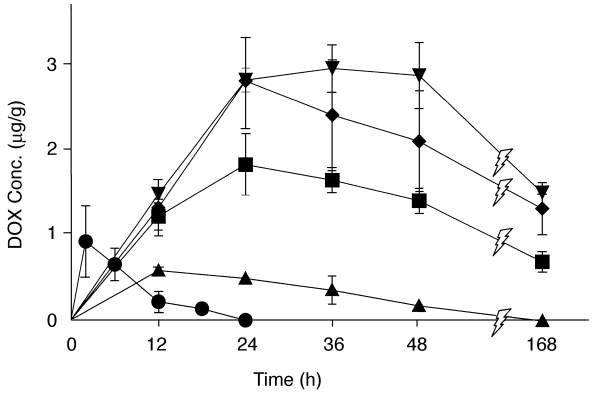

Fig. 4. Concentration of doxorubicin (DOX) in OVCAR-3 carcinoma xenografts in nu/nu mice after intravenous (i.v.) bolus injection of free DOX (●) or P-DOX of different mol. wts: 22 kDa (▲); 160 kDa (■); 895 kDa (◆); 1230 kDa (▼).

Table 2
Doxorubicin (DOX) levels in tissues (μg/g) after i.v. administration of free DOX to nu/nu mice

Sample[a]	Time				
	2 h	6 h	12 h	18 h	24 h
Heart	6.9±0.4	5.9±0.6	4.5±0.5	1.3±0.4	0.3±0.1
Kidney	2.4±0.4	1.9±0.4	1.0±0.3	0.6±0.1	0.2±0.1
Liver	4.8±1.0	4.4±0.8	4.1±0.9	3.0±0.6	1.8±0.5
Lung	4.0±0.8	2.6±0.4	1.4±0.2	0.4±0.1	0.1±0.1
Spleen	4.6±0.7	5.3±0.6	4.3±0.8	2.5±0.7	0.6±0.1

[a] Values are means± standard deviation.

Table 3
Doxorubicin (DOX) levels in tissues (μg/g) after intravenous (i.v.) administration of P-DOX (mol. wt = 22 kDa) to nu/nu mice

Sample[a]	Time				
	12 h	24 h	36 h	48 h	168 h
Heart	0.85±0.3	0.3±0.3	0.1±0.1	0.02±0.01	0.01±0.04
Kidney	0.64±0.1	0.43±0.05	0.5±0.4	0.29±0.03	0.01±0.01
Liver	8.5±1.32	5.4±0.59	5.1±0.61	3.1±0.4	0.1±0.01
Lung	1.63±0.4	1.45±0.5	1.51±0.1	0.13±0.08	0.1±0.01
Spleen	4.5±0.8	2.6±0.6	2.3±0.4	2.1±0.4	0.1±0.02

[a] Values are means ± standard deviation.

Table 4
Doxorubicin (DOX) levels in tissues (μg/g) after intravenous (i.v.) administration of P-DOX (mol. wt = 160 kDa) to nu/nu mice

Sample[a]	Time				
	12 h	24 h	36 h	48 h	168 h
Heart	1.29±0.32	1.88±0.56	1.44±0.13	0.93±0.17	0.09±0.11
Kidney	0.78±0.1	0.95±0.2	0.7±0.2	0.5±0.15	0.13±0.07
Liver	13.2±1.8	17.6±1.6	7.6±0.8	6.8±0.5	1.0±0.12
Lung	1.69±0.3	2.15±0.6	1.79±0.5	0.7±0.1	0.18±0.06
Spleen	8.6±1.5	10.3±1.3	6.5±1.6	5.8±0.9	0.41±0.08

[a] Values are means ± standard deviation.

Table 5
Doxorubicin (DOX) levels in tissues (μg/g) after i.v. administration of P-DOX (mol. wt = 895 kDa) to nu/nu mice

Sample[a]	Time				
	12 h	24 h	36 h	48 h	168 h
Heart	2.98±0.64	1.88±0.88	2.01±0.26	1.09±0.16	0.09±0.13
Kidney	1.12±0.25	1.13±0.3	0.94±0.36	0.7±0.1	0.34±0.07
Liver	18.5±1.8	18.4±2.0	12.1±1.1	8.4±1.06	1.1±0.01
Lung	2.18±0.41	2.28±0.21	2.11±0.31	0.81±0.45	0.23±0.13
Spleen	8.3±1.8	10.2±1.8	6.3±0.85	6.1±0.6	0.6±0.1

[a] Values are means ± standard deviation.

Table 6
Doxorubicin (DOX) levels in tissues (μg/g) after intravenous (i.v.) administration of P-DOX (mol. wt = 1230 kDa) to nu/nu mice

Sample[a]	Time				
	12 h	24 h	36 h	48 h	168 h
Heart	3.3±0.24	2.31±0.2	2.01±0.5	1.46±0.15	0.1±0.02
Kidney	1.3±0.26	1.3±0.25	1.1±0.13	0.8±0.22	0.2±0.01
Liver	23.7±2.2	19.1±1.4	13.2±1.1	9.6±1.6	1.1±0.1
Lung	2.3±0.34	2.56±0.67	2.27±0.39	0.89±0.18	0.2±0.02
Spleen	12.3±1.6	10.2±1.1	6.9±1.0	7.9±0.41	0.8±0.05

[a] Values are means ± standard devation.

were found between the mice receiving P-DOX at a mol. wt higher than 160 kDa ($P > 0.1$). Complete tumour growth regression, toxicity-induced death, significant weight loss or changes in the activity level did not occur in any experimental groups. No obvious changes in the heartbeat rate were observed (data not shown).

4. Discussion

It is now well accepted that the EPR effect is the predominant mechanism by which soluble macromolecular anticancer drugs exert their therapeutic effect on solid tumours [5,8]. The phenomenon is attributed to the high vascular density of the tumour, increased permeability of tumour vessels, defective tumour vasculature and defective or suppressed lymphatic drainage in the tumour interstitium [5]. A number of studies showed increased accumulation of macromolecules in tumours compared with that in normal tissues [5,6,8,13]. The degree of accumulation was dependent on the mol. wt [5], charge [14] and overall hydrophobic–hydrophilic character. The tumour type and micro-environment may influence its transport characteristics (pore cut-off size) [15]. In addition, it appears that differences in tumour morphology after exposure to inert or cytotoxic macromolecules may dramatically influence the intratumour distribution of macromolecules [13,16]. This may have an important impact on the EPR effect with concomitant changes in therapeutic efficacy.

The antitumour activity of HPMA copolymer–doxorubicin conjugates has been demonstrated in various tumour models including Neuro 2A neuroblastoma [17], and human ovarian carcinomas OVCAR-3 [11,12] and A2780 [13]. The effects of mol. wt and administration route of HPMA copolymers on their biodistribution and tissue uptake rate have been examined both *in vitro* and *in vivo* [18–20]. The fate of polymeric drug carriers in the organism is related to their molecular weight [9,20,21]. Polymeric carriers with a molecular weight below the renal threshold may be rapidly lost from circulation. An increase of mol. wt of polymeric drug carriers may result in an increased intravascular half-life with a concomitant increase of therapeutic efficacy [3,7,18–20, 22].

To evaluate the relationship between the mol. wt on tumour accumulation and the bioactivity of P-DOX, novel long-circulating P-DOX conjugates were designed and synthesised [10]; their biodistribution and therapeutic efficacy were evaluated in human ovarian OVCAR-3 xenografts in nude mice. A new crosslinking agent, N^2,N^5-bis(N-methacryloylglycylphenylalanylleucylglycyl)ornithine methyl ester, was synthesised and high-molecular weight HPMA copolymers were prepared by crosslinking copolymerisation below the gel point [1,10]. In contrast to crosslinking of polymer precursors [18–20], this method [10] permits the reproducible synthesis of branched, water-soluble HPMA copolymer–DOX conjugates with a variable range of mol. wts yet without the long-term accumulation of the

conjugate in the host. Both the side-chain terminating in DOX [3,23] and oligopeptide crosslinks are susceptible to cleavage by lysosomal enzymes [3,23,24]. Consequently, the *in vivo* fate may be as follows. Long-circulating P-DOX conjugates are internalised by endocytosis and ultimately will be localised in secondary lysosomes. In the lysosomal compartment, both side-chains and oligopeptide crosslinks are cleaved by lysosomal enzymes releasing free DOX [3] and primary HPMA copolymer chains [22,24]. Following cell death the polymeric carrier can reach the circulation since the mol. wt distribution of the primary chains is below the renal threshold and the carrier structure is such that non-specific interactions with cells will not occur. Consequently, the recapture rate is negligible and the polymeric carrier will be eliminated by glomerular filtration [9].

In agreement with the above discussed phenomena, the *in vivo* fate of long-circulating P-DOX in mice was mol. wt-dependent, and significantly different from free DOX. The clearance rate of P-DOX from the blood (Fig. 3) was mol. wt-dependent and much slower than that of free DOX in accordance with previously published data [6,19]. The long-circulating P-DOX conjugates exhibited a shorter $t_{1/2}$ in blood (Fig. 3) than linear HPMA copolymers at a similar mol. wt [21]. The differences in the mol. wt distribution of the samples tested may be responsible. The long-circulating P-DOX in this study possessed a wide mol. wt distribution, whereas the samples used in the previous study [21] were fractions with a narrow mol. wt distribution. Macromolecular therapeutics with a wider mol. wt distribution contain low mol. wt fractions which are preferentially cleared from the bloodstream resulting in a continuous increase of the mol. wt distribution of the macromolecules remaining in the bloodstream [22].

While the concentration of P-DOX in the blood (after a single i.v. injection) decreased to insignificant levels after 7 days (168 h) for all samples tested, the accumulation of P-DOX in the tumours, as demonstrated in Fig. 4, increased with increasing mol. wt. High levels of DOX continued to exist in the tumours during the first 48 h after i.v. administration of P-DOX; on the contrary, minimal levels of DOX were detectable at 24 h after the mice received free DOX. The time to reach a peak level shifted from 12 to 36 h as the mol. wt of P-DOX increased from 22 to 1230 kDa (Fig. 4). This may indicate a slower extravasation of higher mol. wt conjugates at the tumour site.

The results are consistent with the absorption model analysis. The absorption rate of free DOX is faster than P-DOX (Fig. 5); consequently, free DOX reaches a peak concentration earlier than P-DOX [6]. However, owing to its rapid elimination rate, free DOX merely exhibited a short retention time in the tumours. In contrast, the conjugation of DOX to the HPMA copolymer decreased both the accumulation and elimination rates, resulting in a longer time interval to reach peak levels and an extended retention time in the tumours (larger AUC). This extended residence time of P-DOX in the tumours may contribute to the higher efficacy of macromolecular therapeutics to treat tumours (Fig. 6) when compared with free drugs [13,16,17]. The results also imply that it is possible to manipulate the peak level of P-DOX in tumours by controlling the mol. wt.

As summarised in Tables 2–6, more than 20% of the total administered dose of long-circulating P-DOX (mol. wt $\geqslant$ 160 kDa) was accumulated in the liver at 24 h after i.v. administration; the accumulated amount depended on the mol. wt of P-DOX. This is consistent with our previous results [6]. It is important to note that perfusion of the liver (and other organs) was not performed. Consequently, the high blood content in the liver contributed to the high level of accumulation detected [6]. Since the spleen has physiological properties similar to those of the liver, it may accumulate HPMA copolymer-bound drugs at a similar level. A similar amount of P-DOX accumulated in the kidneys and lungs when compared with free drug.

The conjugation of DOX to HPMA copolymers decreased the accumulation in the heart and did not influence the rate of the heartbeat (data not shown). This is an important observation since cardiotoxicity is one of the main side-effects of DOX therapies [25].

The enhanced accumulation of long-circulating HPMA copolymer–DOX conjugates in tumours may result in a higher efficacy in the treatment of tumours. As shown in Fig. 4, high levels of DOX continued to exist in the tumours during the first 48 h after i.v. administration of long-circulating conjugates; the higher the mol. wt of conjugate, the higher the tumour accumulation. In contrast, minimal levels of DOX were detectable at 24 h after the mice received free DOX. Conjugation of DOX to long circulating HPMA copolymers resulted in an up to 45 times higher AUC for the highest mol. wt P-DOX compared with free DOX (Fig. 4). The higher tumour accumulation resulted in an enhanced therapeutic efficacy (Fig. 6). The comparison of data in Figs. 4 and 6 strongly suggests that the EPR effect [16,26–28] was responsible for the mol. wt-dependent accumulation and efficacy of the long-circulating P-DOX conjugates. The data seem to indicate that higher mol. wt P-DOX possess a greater therapeutic index than P-DOX of lower mol. wts. No mol. wt-related non-specific toxicity was observed in this study. Incorporating antibodies [29–31] or antibody fragments [32], specific for antigens expressed on human ovarian carcinoma cells, into these conjugates would result in a further enhancement of their therapeutic efficacy.

In summary, we conducted this study to compare the accumulation of free and HPMA copolymer-bound DOX in blood and various tissues, especially to char-

acterise the relationship between the mol. wt of the conjugates and their biodistribution and efficacy. We have demonstrated that the newly designed crosslinker permitted the synthesis of P-DOX with mol. wts up to 1230 kDa. The resulting long-circulating P-DOX exhibited a prolonged $t_{1/2}$ in the blood with a concomitant increase in tumour accumulation through the EPR effect. The therapeutic efficacy increased as the mol. wt of P-DOX increased. The low residual concentration of P-DOX in tissues (except tumours) avoids potential long-term side-effects. Additional studies will be required to fully characterise the uptake of P-DOX in the interstitium of tumours, and the ultimate mechanisms of cytotoxicity. The results obtained are promising and clearly warrant clinical investigation of these novel long-circulating conjugates in future applications for the treatment of human ovarian carcinomas.

Acknowledgements

We thank Dr Antonio Suarato for the kind gift of doxorubicin. The research described here was supported in part by the NIH grant CA51578 from the National Cancer Institute.

References

1. Kopeček J, Kopečková P, Minko T, Lu ZR. HPMA copolymer–anticancer drug conjugates: design, activity, and mechanism of action. *Eur J Pharm Biopharm* 2000, **50**, 61–81.
2. Putnam D, Kopeček J. Polymer conjugates with anticancer activity. *Adv Polym Sci* 1995, **122**, 55–123.
3. Kopeček J, Rejmanová P, Strohalm J, *et al*. Synthetic polymeric drugs. U.S. Pat. 5,037,883 (Aug. 6, 1991).
4. Vasey PA, Twelves C, Kaye SB, *et al*. Phase I clinical and pharmacokinetic study of PK1 (HPMA copolymer–doxorubicin): first member of a new class of chemotherapeutic agents — drug–polymer conjugates. *Clin Cancer Res* 1999, **5**, 83–94.
5. Noguchi Y, Wu J, Duncan R, *et al*. Early phase tumor accumulation of macromolecules: a great difference in clearance rate between tumor and normal tissues. *Jpn J Cancer Res* 1998, **89**, 307–314.
6. Shiah JG, Sun Y, Peterson CM, Kopeček J. Biodistribution of free and N-(2-hydroxypropyl)methacrylamide copolymer-bound mesochlorin e_6 and adriamycin in nude mice bearing human ovarian carcinoma OVCAR-3 xenografts. *J Control Rel* 1999, **61**, 145–157.
7. Bogdanov A Jr, Wright SC, Marecos EM, *et al*. A long-circulating co-polymer in 'passive targeting' to solid tumors. *J Drug Target* 1997, **4**, 321–330.
8. Maeda H, Seymour LW, Miyamoto Y. Conjugates of anticancer agents and polymers: advantages of macromolecular therapeutics in vivo. *Bioconjugate Chem* 1992, **3**, 351–355.
9. Šprincl L, Exner J, Šterba O, Kopeček J. New types of synthetic infusion solutions. III. Elimination and retention of poly[N-(2-hydroxypropyl)methacrylamide] in a test organism. *J Biomed Mater Res* 1976, **10**, 953–963.
10. Dvořák M, Kopečková P, Kopeček J. High-molecular weight HPMA copolymer–adriamycin conjugates. *J Control Rel* 1999, **60**, 321–332.
11. Peterson CM, Lu JM, Sun Y, *et al*. Combination chemotherapy and photodynamic therapy with N-(2-hydroxypropyl)methacrylamide copolymer-bound anticancer drugs inhibit human ovarian carcinoma heterotransplanted in nude mice. *Cancer Res* 1996, **56**, 3980–3985.
12. Shiah JG, Sun Y, Peterson CM, Straight RC, Kopeček J. Antitumor activity of N-(2-hydroxypropyl)methacrylamide copolymer-mesochlorin e_6 and adriamycin conjugates in combination therapy. *Clin Cancer Res* 2000, **6**, 1008–1015.
13. Minko T, Kopečková P, Kopeček J. Efficacy of the chemotherapeutic action of HPMA copolymer-bound doxorubicin in a solid tumor model of ovarian carcinoma. *Int J Cancer* 2000, **86**, 108–117.
14. Tabata Y, Kawai T, Murakami Y, Ikada Y. Electric charge influence of dextran derivatives on their tumor accumulation after intravenous injection. *Drug Delivery* 1997, **4**, 213–221.
15. Hobbs SK, Monsky WL, Yuan F, *et al*. Regulation of transport pathways in tumor vessels: role of tumor type and microenvironment. *Proc Natl Acad Sci USA* 1998, **95**, 4607–4612.
16. Minko T, Kopečková P, Pozharov V, Jensen K, Kopeček J. The influence of cytotoxicity of macromolecules and of VEGF gene modulated vascular permeability on the enhanced permeability and retention effect in resistant solid tumor. *Pharmaceut Res* 2000, **17**, 505–514.
17. Krinick NL, Sun Y, Joyner D, Spikes JD, Straight RC, Kopeček J. A polymeric drug delivery system for the simultaneous delivery of drugs activatable by enzymes and/or light. *J Biomater Sci Polym Ed* 1994, **5**, 303–324.
18. Cartlidge SA, Duncan R, Lloyd JB, Rejmanová P, Kopeček J. Soluble, crosslinked N-(2-hydroxypropyl)methacrylamide copolymers as potential drug carriers. 1. Pinocytosis by rat visceral yolk sacs and rat intestine cultured *in vitro*. Effect of molecular weight on uptake and intracellular degradation. *J Control Rel* 1986, **3**, 55–66.
19. Cartlidge SA, Duncan R, Lloyd JB, Kopečková-Rejmanová P, Kopeček J. Soluble, crosslinked N-(2-hydroxypropyl)methacrylamide copolymers as potential drug carriers. 2. Effect of molecular weight on blood clearance and body distribution in the rat after intraveneous administration. Distribution of unfractionated copolymer after intraperitoneal, subcutaneous or oral administration. *J Control Rel* 1987, **4**, 253–264.
20. Cartlidge SA, Duncan R, Lloyd JB, Kopečková-Rejmanová P, Kopeček J. Soluble, crosslinked N-(2-hydroxypropyl)methacrylamide copolymers as potential drug carriers. 3. Targeting by incorporation of galactosamine residues. Effect of route of administration 2. *J Control Rel* 1987, **4**, 253–264.
21. Seymour LW, Duncan R, Strohalm J, Kopeček J. Effect of molecular weight (M_W) of N-(2-hydroxypropyl)methacrylamide copolymers on body distribution and rate of excretion after subcutaneous, intraperitoneal, and intravenous administration to rats. *J Biomed Mater Res* 1987, **21**, 1341–1358.
22. Kopeček J, Cífková I, Rejmanová P, Strohalm J, Obereigner B, Ulbrich K. Polymers containing enzymatically degradable bonds. 4. Preliminary experiments in vivo. *Makromol Chem* 1981, **182**, 2941–2949.
23. Rejmanová P, Pohl J, Baudyš M, Kostka V, Kopeček J. Polymers containing enzymatically degradable bonds. 8. Degradation of oligopeptide sequences in N-(2-hydroxypropyl)methacrylamide copolymers by bovine spleen cathepsin B. *Makromol Chem* 1983, **184**, 2009–2020.
24. Šubr V, Kopeček J, Pohl J, Baudyš M, Kostka V. Cleavage of oligopeptide side-chains in N-(2-hydroxypropyl)methacrylamide copolymers by mixtures of lysosomal enzymes. *J Control Rel* 1988, **8**, 133–140.
25. Yeung TK, Hopewell JW, Simmonds RH, *et al*. Reduced cardiotoxicity of doxorubicin given in the form of N-(2-hydroxypropyl)methacrylamide conjugates: an experimental study in the rat. *Cancer Chemother Pharmacol* 1991, **29**, 105–111.
26. Jain RK. Delivery of molecular and cellular medicine to solid tumors. *Microcirculation* 1997, **4**, 1–23.

27. Baish JW, Gazit Y, Berk DA, Nozue M, Baxter LT, Jain RK. Role of tumor vascular architecture in nutrient and drug delivery: an invasion percolation-based network model. *Microvasc Res* 1996, **51**, 327–346.
28. Yeo KT, Wang HH, Nagy JA, Dvorak AM. Vascular permeability factor (vascular endothelial growth factor) in guinea pig and human tumor and inflammatory effusions. *Cancer Res* 1993, **53**, 2912–2919.
29. Omelyanenko V, Gentry C, Kopečková P, Kopeček J. HPMA copolymer–anticancer drug–OV-TL16 antibody conjugates. 2. Processing in epithelial ovarian carcinoma cells in vitro. *Int J Cancer* 1998, **75**, 600–608.
30. Sjögren HO, Isaksson M, Willner D, Hellström I, Hellström KE, Trail PA. Antitumor activity of carcinoma-reactive BR96–doxorubicin conjugate against human carcinomas in athymic mice and rats and syngeneic rat carcinomas in immunocompetent rats. *Cancer Res* 1997, **57**, 4530–4536.
31. Říhová B, Jelínková M, Strohalm J, *et al*. Polymeric drugs based on conjugates of synthetic and natural macromolecules. II. Anticancer activity of antibody or $(Fab')_2$ conjugates and combined therapy with immunomodulators. *J Control Rel* 2000, **64**, 241–261.
32. Lu ZR, Kopečková P, Kopeček J. Polymerizable Fab' antibody fragments for targeting of anticancer drugs. *Nature Biotechnol* 1999, **17**, 1101–1104.